Synthesis, Material Properties, and Organocatalytic Performance of Hypervalent Iodine(III)-Oxidants in Core–Shell-Structured Magnetic Nanoparticles

Julien Grand, Carole Alayrac, Simona Moldovan, Bernhard Witulski

catalysts

MDPI

Article

Synthesis, Material Properties, and Organocatalytic Performance of Hypervalent Iodine(III)-Oxidants in Core–Shell-Structured Magnetic Nanoparticles

Julien Grand [1], Carole Alayrac [1], Simona Moldovan [2] and Bernhard Witulski [1,*]

[1] Laboratoire de Chimie Moléculaire et Thio-Organique (LCMT), CNRS UMR 6507, ENSICAEN, Université de Caen, Normandie Univ., 6 Bd. Maréchal Juin, 14050 Caen, France
[2] Groupe de Physique des Matériaux (GPM), CNRS UMR 6634, INSA & Université Rouen, Normandie Univ., 76000 Rouen, France; simona.moldovan@univ-rouen.fr
* Correspondence: bernhard.witulski@ensicaen.fr

Abstract: Magnetic nanoparticles (MNPs) based on magnetite (Fe_3O_4) are attractive catalyst supports due to their high surface area, easy preparation, and facile separation, but they lack stability in acidic reaction media. The search for MNPs stable in oxidative acidic reaction media is a necessity if one wants to combine the advantages of MNPs as catalyst supports with those of iodine(III) reagents being environmentally benign oxidizers. In this work, immobilized iodophenyl organocatalysts on magnetite support (IMNPs) were obtained by crossed-linking polymerization of 4-iodostyrene with 1,4-divinylbenzene in the presence of MNPs. The obtained IMNPs were characterized by TGA, IR, SEM, STEM, and HAADF to gain information on catalyst morphology, average particle size (80–100 nm), and their core–shell structure. IMNP-catalysts tested in (i) the α-tosyloxylation of propiophenone **1** with *meta*-chloroperbenzoic acid (*m*-CPBA) and (ii) in the oxidation of 9,10-dimethoxyanthracene **3** with Oxone® as the side-oxidant showed a similar performance as reactions using stoichiometric amounts of iodophenyl. The developed IMNPs withstand strong acidic conditions and serve as reusable organocatalysts. They are recyclable up to four times for repeated organocatalytic oxidations with rates of recovery of 80–92%. This is the first example of a—(4-iodophenyl)polystyrene shell—magnetite core-structured organocatalyst withstanding strong acidic reaction conditions.

Keywords: organocatalysis; oxidation; hypervalent iodine; magnetic nanoparticles; sustainable source; core–shell-structured materials; polymer

Citation: Grand, J.; Alayrac, C.; Moldovan, S.; Witulski, B. Synthesis, Material Properties, and Organocatalytic Performance of Hypervalent Iodine(III)-Oxidants in Core–Shell-Structured Magnetic Nanoparticles. *Catalysts* **2024**, *14*, 677. https://doi.org/10.3390/catal14100677

Academic Editor: Werner Oberhauser

Received: 13 September 2024
Revised: 22 September 2024
Accepted: 24 September 2024
Published: 1 October 2024

1. Introduction

Hypervalent iodine(III) reagents are frequently used in selective oxidative transformations of organic molecules of pharmaceutical or material interest. They progressively emerge to replace toxic and environmentally problematic heavy metal oxidants. Chemical transformations involving iodine(III) reagents not only comprise simple oxidations, they are further capable to induce oxidative carbon–carbon or carbon–heteroatom bond formations. Moreover, they can persuade molecular skeleton rearrangements in suitable organic substrates via iodine(III)-mediated reaction cascades. The chemistry of polyvalent iodine reagents, including synthesis and applications in chemo-, stereo-, or enantioselective oxidative transformations, has progressed rapidly during recent years and is regularly up-dated in reviews and book chapters [1–9].

Our interest in hypervalent iodine(III) compounds lies in their potential for being chemoselective environmentally benign oxidants for organic chemical transformations. However, most of the procedures involving iodine(III) reagents rely on their stoichiometric use. More recently, organocatalytic processes with sub-stoichiometric amounts of iodine(III) reagent/catalyst have emerged. Here, the iodine reagent is in

situ re-oxidized by a side-oxidant [10–14]. Another issue for increasing efficiency while reducing the costs of hypervalent iodine(III) reagents is their modification for potential recyclability and reuse [15]. Recycling of the iodine(III) reagents is a task of great economic and environmental importance, not only for organic synthesis but also for chemical and pharmaceutical industries. Reported recyclable hypervalent iodine(III) reagents include phenyliodo(diacetate) (PIDA) moieties supported on polymers [16–28], ionic liquid-supported PIDA-type reagents [29–36], fluoroalkane functionalized iodine(III) reagents [37–40], polyarenes [41–45], and other functionalized iodine(III) reagents isolable by crystallization or acid/base extraction [7,15].

The development of iodine(III) reagents on magnetic supports is less well investigated. Magnetite (Fe_3O_4) nanoparticle-supported (diacetoxyiodo)benzene (DIB), where the iodine(III) reagent is immobilized via an organosilane connection, has been used for the batch-wise oxidation of primary and secondary alcohols in the presence of 2,2,6,6-tetramethylpiperidine-1-oxyl (TEMPO) to yield aldehydes and ketones, respectively [46]. The TEMPO/iodine(III) system was also used in the selective oxidation of benzyl alcohols to benzaldehydes using a recyclable magnetite polyaniline nanocomposite containing hypervalent iodine(III) moieties [47]. However, both magnetite-supported hypervalent iodine reagents for alcohol oxidations did not succeed organocatalytic versions or reaction protocols with sub-stoichiometric amounts of magnetite-supported catalyst and side-oxidants for re-activating iodine-catalyst sides. More recently, the oxidation of 4-alkoxyphenols to quinones using magnetite particle-supported iodoarenes as the catalyst and Oxone® as the side-oxidant has been reported [48]. Iodine(III) catalysts attached to the magnetite core via phosphonic acid coating were more stable than their silane counterparts. Notably, the procedure needed careful adjustment of the reaction solution with a 0.1 M phosphate buffer to avoid strong acid conditions that induced decomposition of the magnetite (Fe_3O_4) support.

Immobilization of catalysts on solid and/or polymer support allows merging the principles of quasi-homogeneous phase catalysis with the advantages of heterogeneous catalysis when it comes to the point of easy catalyst recovery. To counteract the problem of a lower accessibility of solid bound catalysts, the size of the catalyst support might be reduced to the nanometer dimension, as this will increase the active surface area and realize quasi-homogeneous catalysis conditions. However, such a reduced particle size will make catalyst separation by filtration or centrifugation less facile. Here, the use of magnetite (Fe_3O_4) nanoparticles (MNPs)—which become magnetic in the presence of an external magnetic field—is of great interest, as their separation from a reaction solution is operationally simple; MNPs are collectable after a chemical transformation with a strong permanent magnet [49–59]. However, readily available nanometer-sized magnetite (Fe_3O_4) nanoparticles as supports have severe drawbacks; mainly, they possess insufficient stability in both acidic and basic media. One promising method to gain higher stability of the magnetite core is to use a polymer shell acting as impenetrable protection shield [60–62]. Such an assembly, in its idealized form, results in a core–shell structure with a magnetite core surrounded by a functionalized polymer shell containing iodophenyl moieties and acting as the organocatalyst.

Objectives of our present work are (i) the development of magnetite nanoparticle-supported iodoarene containing core–shell-structured catalysts suitable for organocatalytic oxidation reactions; (ii) their characterization concerning morphology, particle size, and core–shell structure; (iii) their use in truly organocatalytic oxidations involving in situ-formed hypervalent iodine(III) catalytic sides; and (iv) proof of concept that those newly developed organocatalysts are easily separable, reusable, and notably stable in strong acid reaction media.

2. Results and Discussion

Aiming to develop recyclable hypervalent iodine(III) organocatalysts on the basis of magnetite nanoparticles with a core–shell architecture, we investigated iodophenyl functionalized polystyrene covering magnetite nanoparticles (IMNPs). The synthesis

of cross-linked polystyrene was chosen to ensure a long-term stability of the resulting polystyrene/MNP blend in acidic reaction media. First attempts of a post-functionalization of readily available polystyrene–magnetite core–shell nanoparticles by iodination of polystyrene phenyl units, however, were unsuccessful. The obtained degree of iodophenyl moieties was too low to realize suitable organo-catalytic processes. We therefore switched our strategy of synthesis to directly implement the iodoaryl function, which later will serve as the iodine(III)-based organocatalyst, via cross-linking polymerization of 4-iodostyrene with 1,4-divinylbenzene in the presence of magnetite MNPs to obtain the desired IMNPs.

2.1. Synthesis of Iodinated Core–Shell Type Magnetic Nanoparticles (IMNPs)

The synthesis of IMNPs used in our study is outlined in Scheme 1. Magnetite (Fe_3O_4) nanoparticles were prepared by alkaline hydrolysis of ferric [Fe(II)] and ferrous [Fe(III)] chloride in aqueous phase at 90 °C via syringe pump addition (20 mL/h). Magnetite (Fe_3O_4) has ferromagnetic properties due to the two iron valence states, Fe^{2+} and Fe^{3+}. Each nanoparticle performs as a single magnetic domain in the presence of an external magnetic field and due to a low remanence and coercivity, magnetization returns back to the non-magnetized state when the external magnetic field is removed [63].

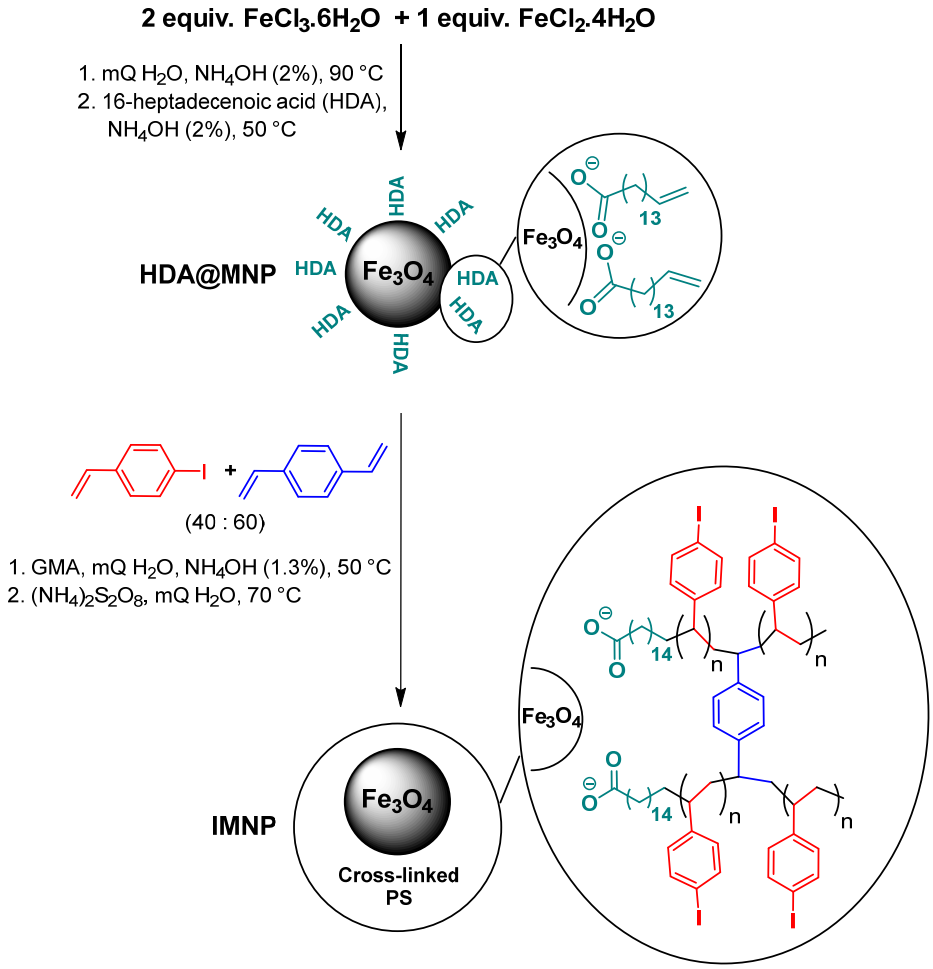

Scheme 1. Preparation of Fe_3O_4-based magnetic nanoparticles stabilized with 16-heptadecenoic acid (HDA@MNP) and their conversion to "core–shell-structured" iodinated magnetic nanoparticles (IMNPs).

Once formed MNPs were collected with a permanent magnet, they were washed and stabilized by adding 16-heptadecenoic acid in an aqueous solution of ammonium hydroxide to give HDA@MNPs. The latter were encapsulated via cross-linking emulsion polymerization of 4-iodostyrene and 1,4-divinylbenzene, initiated by ammonium persulfate

to give the desired IMNPs. 16-Heptadecenoic acid served both as MNP stabilizer and as linker between the iron oxide core and the formed polymer shell. A high cross-linking degree was secured by using a molar ratio of 40:60 for 4-iodostyrene to 1,4-divinylbenzene. At the end of the reaction, IMNPs were collected with the help of an external permanent magnet and washed with water, methanol, and dichloromethane and dried in vacuum. The obtained IMNPs disperse in solution using a shaking plate and are easily collected, separated, and recovered from the supernatant reaction solution with the help of an external permanent magnet. In the literature, it is noted that core–shell-structured magnetite particles show a small decrease of saturation magnetization, which can be attributed to the mass percentage of the organic shell [64]. However, in our study this is negligible, as it does not influence the high recovery rate with an external magnet, as shown with the IMNPs of this study in Figure 1.

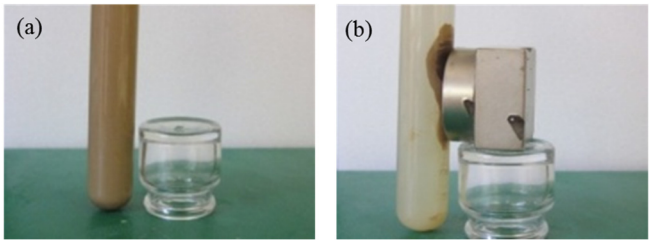

Figure 1. Reaction mixture containing (**a**) dispersed IMNPs in the absence of an external magnet and (**b**) IMNPs collected using an external permanent magnet.

2.2. Characterization of Core–Shell Type IMNPs by Analytical and Spectroscopic Means

Thermo-gravimetric analysis (TGA) of thus obtained IMNPs reveals their thermal stability up to 270 °C. At higher temperatures, decomposition of the organic polymer begins. The combustion process is complete at temperatures superior to 500 °C. Based on TGA results, the obtained IMNPs show a 50% loss of weight that corresponds to polymeric organic material (see Supplementary Materials). Furthermore, the number of accessible iodine functions in the IMNPs was determined via iodometric titration, indicating a phenyl iodine load of 0.63 mmol/g of IMNP (see Supplementary Materials).

The X-ray diffraction pattern (XRD) of magnetite nanoparticles (MNPs) and obtained IMNPs are shown in Figure 2A. Sites and intensities of MNP and IMNP diffraction peaks are consistent and match those of standard patterns for bulk magnetite Fe_3O_4 (JCPDS File no. 19-0629) [65]. Concerning the XRD of IMNPs, all diffraction planes correspond to the parent MNPs and reveal conservation and stability of the core magnetite structure. The amorphous peak around 20° being only present in IMNPs is attributed to the diffuse polystyrene shell.

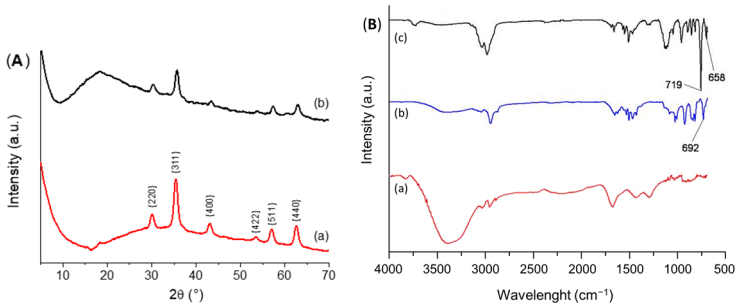

Figure 2. (**A**) Powder XRD pattern of (a) magnetite nanoparticles (MNPs) and (b) iodinated core-shell-structured magnetic nanoparticles (IMNPs); (**B**) ATR-FT-IR spectra of (a) MNPs, (b) HDA@MNPs, and (c) IMNPs.

Figure 2B compiles powder ATR-FT-IR spectra of MNP, HDA@MNP, and IMNP samples. Grafting of the magnetite cores by 16-heptadecenoic acid was confirmed by IR spectra. The bands from 1600 cm^{-1} to 1300 cm^{-1} are attributed to the υCO_2^- vibration of a carboxylate linked to an iron oxide surface by a bidentate interaction [66], whereas the broad band around 3400 cm^{-1} belongs to the νOH vibration of HDA or water adsorbed to the particle surface. Notably, when the magnetite core is encapsulated into a polystyrene shell, these bands disappear; whereas now, new bands in the region of 800 to 950 cm^{-1} indicate unsaturated CH deformations, being characteristic for substituted benzene derivatives. Bands in the region of 1000 cm^{-1} to 700 cm^{-1} differ significantly in the IR spectra of MNPs, HDA@MNPs, and IMNPs. The intense IR band at 719 cm^{-1} indicates a 4-substituted iodobenzene moiety being present in the IMNPs (see also Supplementary Materials).

2.3. Morphology, Particle Size, and Imaging of IMNPs by SEM and DLS Investigation

Morphology, particle size distribution, and material architecture of synthesized IMNPs were investigated by scanning electron microscopy (SEM) and high-resolution transmission electron microscopy (STEM-HAADF). Obtained data were compared with those from respectively synthesized magnetite MNPs (Figures 3 and 4).

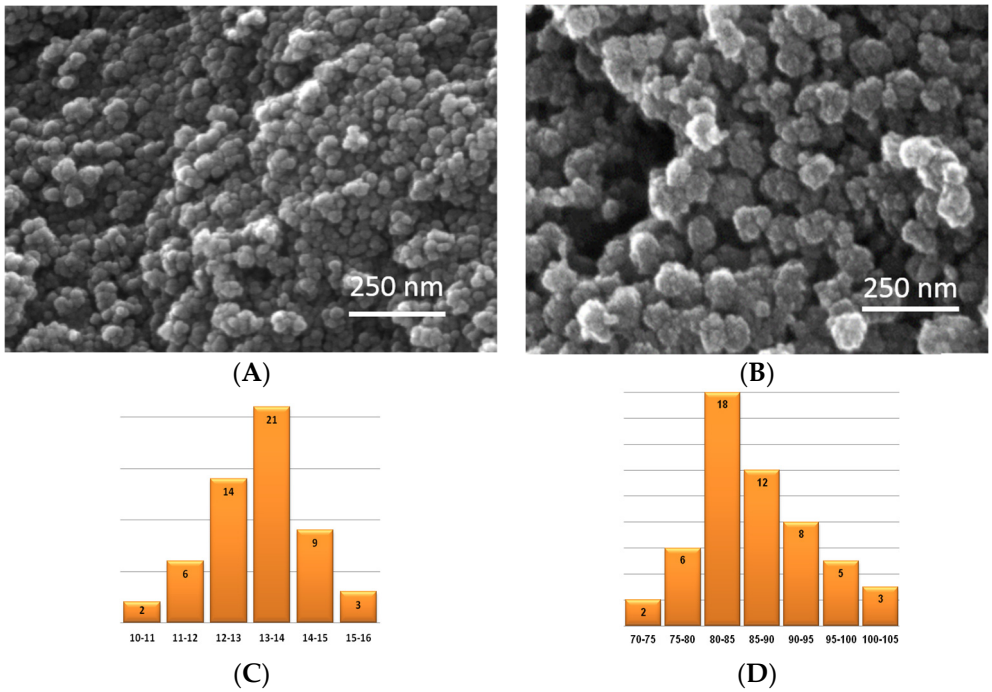

Figure 3. SEM images of obtained (**A**) magnetite MNPs and (**B**) obtained IMNPs (see also Supplementary Materials) together with their particle size distribution histogram for 55 measured particles of (**C**) MNPs and (**D**) IMNPs, as determined from the SEM image.

According to SEM image data depicted in Figure 3B, the obtained IMNPs comprise agglomerated spheres with a rough appearance but a regular structured surface. The average particle size diameter was determined to be 80–85 nm (Figure 3D). Such a six-fold increase in particle size, when compared to the parent magnetite MNPs—which are significantly smaller, with an average particle size of 13–14 nm (Figure 3A,C)—can been seen as an indication of the quasi core–shell architecture of the IMNPs. A comparable increase of particle size could also be observed by DLS measurements, confirming the increase of particle size from HDA@MNP to IMNP (see Supplementary Materials).

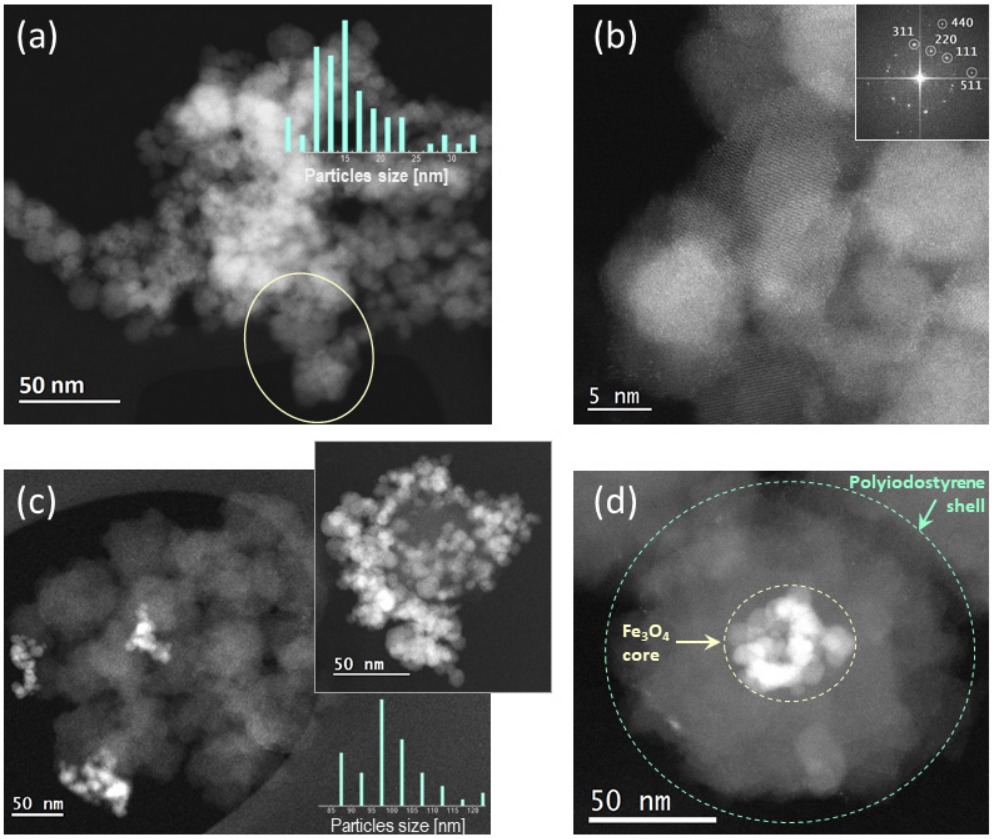

Figure 4. STEM-HAADF micrographs of obtained magnetite MNPs (upper row) and those of IMNPs. (**a**) General view of MNP agglomerations with the size distribution in inset; (**b**) HR-STEM-HAADF image of several MNPs and the FFT in the inset confirm the crystal structure of Fe_3O_4; (**c**) spatial distribution of Fe_3O_4 IMNPs on the polymer granules and statistical size distribution of the polymer; and (**d**) the "idealized core shell structure" of IMNPs.

2.4. TEM Investigations of MNPs and IMNPs

Detailed images of the morphology and structure of MNPs and IMNPs were obtained by STEM-HAADF mode imaging. For this investigation, a double corrected analytical JEOL ARM 200CF TEM in STEM mode has been employed. The use of high-angular annular dark-field (HAADF) STEM was chosen, as in this mode the intensity scales with the Z atomic number of the components, such that high Z elements like the Fe_3O_4-based particles will appear bright when compared to the dark grey level of the carbon-based organic polymer in cases where the latter is present. Figure 4 depicts STEM-HAADF micrographs of the obtained MNPs and IMNPs for reason of comparison.

Figure 4a,b corresponding to the MNPs clearly show the presence of agglomerated but polymer-free magnetite nanoparticles. Particles agglomerate by a few tens up to a few hundreds of nanoparticles. Particle sizes vary from 6 to 35 nm in diameter, as shown by the histogram in the inset of Figure 4a. The sizes of more than 100 NPs have been measured, and their distribution shows that the majority of MNPs have sizes between 13 and 15 nm, with an average overall particle size of 13.5 nm, a value that confirms the average particle size of MNPs determined by SEM. The nanoparticles with sizes superior to 20 nm, such as the ones encircled in Figure 4a, exhibit non-regular shapes with porous-like morphologies marked by the presence of interconnected NPs, with sizes smaller than 6 nm. The high-resolution HR-STEM-HAADF image in Figure 4b confirms the high crystallinity of the magnetite MNPs. The FFT corresponding to the micrograph displayed in the inset allowed the identification of the main crystallographic orientations corresponding to the Fe_3O_4 nanocrystals.

In Figure 4c,d representative STEM-HAADF micrographs of the magnetite/polyiodostyrene composite (IMNPs) are shown. The enhanced chemical contrast between the Fe-based NPs and the carbon-based polymer allows us to undoubtedly locate the Fe_3O_4 NPs (light in the image) against the polyiodostyrene particles (grey quasi-spherical granules). As anticipated by the SEM observations, the particle size is considerably higher after processing, from 80 to 125 nm, with a mean value of 102 nm (histogram in Figure 4c), and the polymer's irregular morphology is clearly visible. The composite magnetite/polyiodostyrene particles are not uniform in shape, and they are best described as polymer flakes with randomly embedded or attached magnetite cores. Agglomerations of Fe_3O_4 MNPs are randomly dispersed on the polymer surface, fixed on the topological asperities, and simply connected to the polymer (see Figure S3 in SI) or embedded into the polyiodostyrene granules (inset in Figure 4c). However, some particles also display the more idealized, ball-shaped, core–shell architecture with a centered magnetite core, as shown in Figure 4d. Here, the particle size is 125 nm, with a core magnetite particle diameter of 37 nm and a shell thickness of 40 nm. The magnetite-rich core is constituted by an agglomeration of interconnected MNPs, with intergranular porosities slightly different than the ones observed for the MNPs in terms of their morphology and compaction. The presence of an Fe_3O_4 core within the composite was confirmed by the STEM-EDS analysis of the core–shell IMNP nanostructure, as shown in Figure S4 (see Supplementary Materials).

2.5. Evaluation of IMNPs as Suitable Organocatalysts for Oxidative Transformations

Performance evaluation of IMNPs as a recyclable iodine(III) reagent and organocatalyst was accomplished with two frequently used hypervalent iodine(III)-mediated transformations, the α-tosyloxylation of propiophenone [67,68] and the oxidation of 9,10-dimethoxyanthracene [69].

2.5.1. α-Tosyloxylation of Propiophenone with IMNPs

The oxidative transformation of propiophenone (**1**) to give the α-tosyloxylated product **2** was executed in acetonitrile at room temperature with three equivalents of *para*-toluenesulfonic acid (*p*-TsOH x H_2O) and three equivalents of *meta*-chloroperbenzoic acid (*m*-CPBA) serving as the side oxidant (Scheme 2). Stoichiometric amounts of either iodobenzene or IMNPs (in relation to accessible iodophenyl moieties determined by iodometry) were used. Both reactions provided the desired product **2** in yields of 87% and 85%, respectively (Table 1, entry 1 and 2). This result indicates that the here-developed IMNPs show a similar catalytic performance to the bare iodophenyl. Importantly, the IMNPs could be fully recovered (98%) after this first run (Table 1, entry 2).

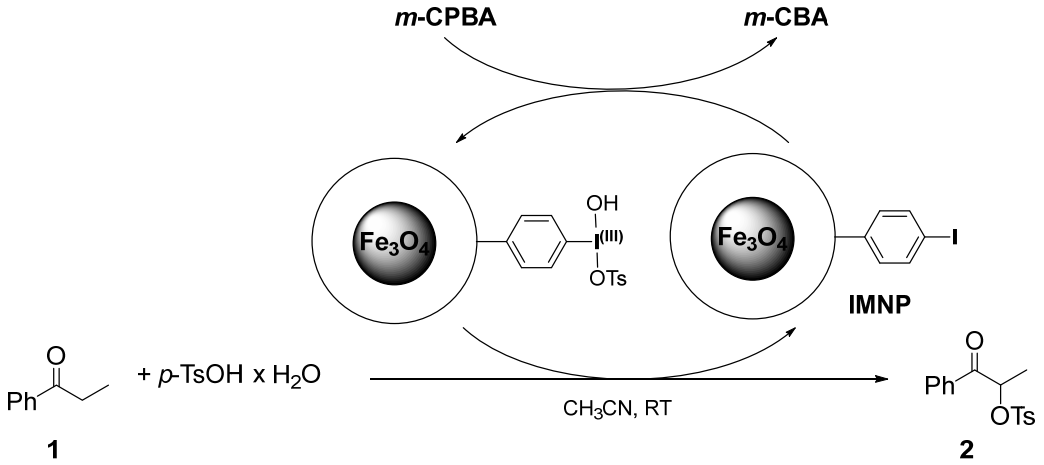

Scheme 2. Organocatalytic α-tosyloxylation of propiophenone (**1**) with IMNPs and *m*-CPBA as the side oxidant to give α-tosyloxypropiophenone **2**.

Table 1. Organocatalytic α-tosyloxylation of propiophenone (**1**) with IMNPs.

Entry	Run	Iodine Source	Yield of 2 [a] [%]	Recovered IMNPs [b] [%]
1	0	iodobenzene	87	-
2	1	IMNPs	85	98
3	2	IMNPs	39	98
4	3	IMNPs	15	91

[a] Yield (mol-%) of isolated compound. [b] Yield (weight-%) of recovered material after being washed with acetonitrile and dried in vacuum.

Such a high rate of recovery of iodine reagent is difficult to achieve with the parent iodobenzene. Moreover, recycling of iodobenzene from the reaction mixture needs strenuous chromatographic methods and is often accompanied by huge material loss in comparison to simple collection of IMNPs with the help of a permanent magnet.

The yield of recovered IMNPs remained high after their second and third reuse, with 98% and 91%, respectively (Table 1, entries 3 and 4). However, after several reuses, the yield of product **2** decreases significantly, with yields of 39% and 15% for the second and third run, respectively. As the rate of recovery of IMNPs was unaffected by its multifold reuse, we assume that accumulated organic compounds (i.e., propiophenone or *para*-toluenesulfonic acid bound to iodine(III) centers) block accessible catalytic sides and might explain the inhibition of catalytic activity. Indeed, TGA analysis of recovered IMNPs indicates a 10 weight-% loss of low molecular weight compounds in the temperature range up to 270 °C in comparison to freshly prepared IMNPs displaying no weight loss below 270 °C (see Supplementary Materials).

2.5.2. IMNP-Mediated Organocatalytic Oxidation of 9,10-Dimethoxyanthracene

The oxidation of 9,10-dimethoxyanthracene (**3**) to give anthraquinone **4** was carried out in trifluoroethanol (TFE) with sub-stoichiometric amounts of IMNPs (30 mol% of accessible iodophenyl moieties) and with Oxone® (4 equivalent) acting as the side-oxidant (Scheme 3). Four consecutive runs with an average yield of 78% of **4** were performed with high rates of recovered (81–97%) IMNPs (Table 2, entries 1–3).

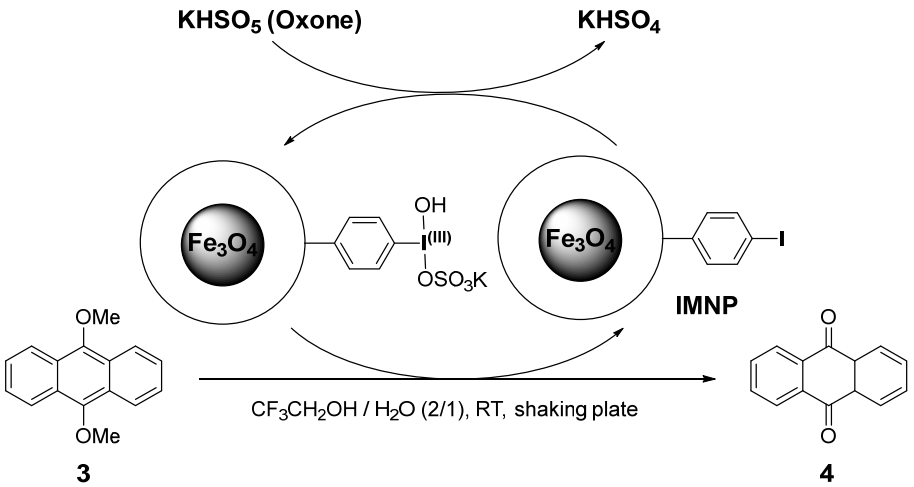

Scheme 3. Organocatalytic oxidation of 9,10-dimethoxyanthracene (**3**) with sub-stoichiometric amounts of IMNPs (30 mol%) and with Oxone® as the side-oxidant to give anthraquinone **4**.

It is important to notice that these reactions were performed using sub-stoichiometric amounts of IMNPs (30 mol%), and the first cycles proceeded with similar efficiencies to those found with stoichiometric amounts of iodobenzene. The latter procedure yielded product **4** at 88% (Table 2, entry 5). Finally, we checked that the oxidation reaction with Oxone® as the side-oxidant is truly catalyzed by the iodophenyl functions of the IMNPs by

running the reaction with bare MNPs as a control (Table 2, entry 6). Under these conditions, only trace amounts of anthraquinone **4** were formed. Most of the MNPs were destroyed under the reaction conditions and lost their magnetite properties. This result clearly states that a stability increase in MNPs is reached under oxidative acidic reaction conditions by protecting them with a polymer shell, where the latter serves both as protective shell and as carrier for the iodophenyl catalyst moiety.

Table 2. Organocatalytic oxidation of 9,10-dimethoxyanthracene (**3**) with IMNPs.

Entry	Run	Reagent (mol%)	Yield of 4 [a] [%]	Recovered IMNPs [b] [%]
1	1	IMNPs (30)	85	97
2	2	IMNPs (30)	77	81
3	3	IMNPs (30)	75	80
4	4	IMNPs (30)	75	92
5	1	Iodobenzene (100)	88	-
6	1	MNP (100)	<10	7

[a] Yield of isolated compound **4**. [b] Yield (weight %) of recovered material after being washed and dried in vacuum.

3. Materials and Methods

Thermo-gravimetric analyses (TGA) were carried out on a SETSYS 1750 CS evolution instrument (SETARAM, Kep Technologies, Mougins, France). Samples were heated from 25 °C to 800 °C with a heating ramp of 5 °C/min (flow rate: 40 mL/min). Powder X-ray diffraction (XRD) patterns were collected with a PANalytical X'Pert Pro diffractometer (Malvern Panalytical Ltd., Malvern, UK) using the Cu Kα radiation (λ = 1.5418 Å, 45 kV, 40 mA). Infrared spectra (IR) were recorded at room temperature on a Perkin Elmer SPECTRUM ONE FT-IR ATR spectrometer (Perkin Elmer, Waltham, MA, USA). Scanning electron microscopy (SEM) was performed with a MIRA-LMH (TESCAN, Brno, Czech Republic) fitted with a field emission gun using an accelerating voltage of 30.0 kV. For dynamic light scattering (DLS) studies (see Supplementary Materials), a Malvern Zetasizer-Nano instrument (Malvern Panalytical Ltd., UK) equipped with a 4 mW He-Ne laser (633 nm) was used. For TEM investigations, a double-corrected analytical JEOL ARM 200CF TEM (JEOL Ltd. Tokyo, Japan) equipped with a 100 mm^2 Centurio detector for the X-rays and a Quantum GIF spectrometer for electron energy loss detection was employed under the Scanning TEM mode. It allowed us to achieve spatial resolutions down to 9 Å in a routine manner and chemical resolutions down to 5 eV in EDS and 0.4 eV in EELS. Prior to the STEM investigations, the sample was dispersed with ultrasound for a few minutes and afterwards drop-casted on a carbon membrane deposited onto a 300 mesh TEM grid. The observations were carried at 80 kV in an effort to minimize the electron beam damage, particularly of the polymer. The STEM-HAADF parameters were used for medium- and high-resolution imaging and STEM EDX (see Supplementary Materials) for assessing the chemical composition. STEM imaging at 80 kV accelerating voltage was used to avoid beam-induced damage; spot size 1 nm; camera length: 8 cm. Imaging: STEM: 1024 × 1024; 19 μs/px. EDS mapping parameters: 256 × 256 px; 0.05 msec/px, drift correction every 60 s.

4. Conclusions

In conclusion, an operationally simple protocol to obtain quasi core–shell-structured magnetic nanoparticles (IMNPs) consisting of a magnetite core as the support and a cross-linked (4-iodophenyl)polystyrene acting as the polymer shell was developed. Their synthesis starts from a magnetite nanoparticle (MNP) preparation with Fe(II)- and Fe(III)chloride, stabilizing them with 16-heptadecenoic acid to HDA@MNP. This was followed by their inclusion into crossed-linked poly(4-iodophenyl)styrene via cross-linking polymerization of 4-iodophenylstyrene and 1,4-divinylbenzene. The obtained IMNPs were characterized in detail by analytical and spectroscopical means. The IMNP particle size was determined

by SEM and STEM imaging, averaging a particle diameter of 80–100 nm, and having a core–shell architecture or MNP clusters attached to polymer flakes, where the acid sensitive magnetite is protected by the (4-iodophenyl)polystyrene. The obtained IMNPs were successfully evaluated in oxidative organocatalysis with either *m*-CPBA or Oxone® as the side-oxidant. The catalytic performance of reused IMNP catalysts is operable in up to four recovery cycles with high degrees of catalyst recovery (80–92%). The main achievement of this study was to demonstrate a concept for stabilizing magnetite as a support for a hypervalent iodine(III)-organocatalyst via a core–shell structure. The obtained core–shell-structured catalysts make them suitable for reactions under strong acid conditions. Notably, another major advantage of the developed protocol lies in the ease of separation of IMNP catalysts from the reaction medium by magnetic separation with the help of an external permanent magnet. This is the first example of a magnetite core–polymer shell-structured iodophenyl organocatalyst withstanding strong acidic reaction conditions that can be used in a truly organocatalytic reaction protocol. Using such IMNPs as organocatalysts will open future possibilities for applications in the field of non-toxic and environmentally benign recyclable hypervalent iodine(III) reagents as oxidizers under strong acidic conditions.

Supplementary Materials: The following supporting information can be downloaded at: https://www.mdpi.com/article/10.3390/catal14100677/s1, Figure S1: Iodometry. Figure S2: Comparison of TGAs of IMNPs used in the *a*-tosylation of propiophenone (**1**). Figure S3: ATR-FT-IR spectra of (a) HDA@MNPs; (b) IMNPs; (c) MNPs; (d) iodobenzene, and (e) benzene. Figure S4: SEM image of MNPs. Figure S5: SEM image of IMNPs. Figure S6: DLS measurements of HDA@MNPs and (b) IMNPs materials. Figure S7: STEM-HAADF micrographs of different regions of the AADF showing the random distribution of the Fe_3O_4 agglomerates of NPs on the polymer surface. Figure S8: STEM-EDS analysis of a core-shell morphology within the IMNPs. See references [70–76].

Author Contributions: Conceptualization, supervision, project administration and funding acquisition, B.W. and C.A.; experimental investigation, data acquisition, and validation, J.G.; TEM investigation and analysis, S.M.; writing—original draft preparation, reviewing, and editing B.W., C.A. and S.M. All authors have read and agreed to the published version of the manuscript.

Funding: This research was supported by CNRS, Conseil Régional de Normandie (France), European FEDER funding, and the French Agence Nationale de la Recherche Labex EMC3 through project ZEOMAH (ANR-10-LABX-09-01). GENESIS is supported by the Région Haute-Normandie, the Métropole Rouen Normandie, and the French National Research Agency as a part of the program "Investissements d'avenir" (ANR-11-EQPX-0020). This work was partly supported by the CNRS federation IRMA–FR 3095.

Data Availability Statement: Data presented in this study are available on request from the authors.

Conflicts of Interest: The authors declare no conflicts of interest.

References

1. Wirth, T. (Ed.) *Hypervalent Iodine Chemistry—Modern Developments in Organic Synthesis*; Topics in Current Chemistry; Springer: Berlin/Heidelberg, Germany, 2003.
2. Tohma, H.; Kita, Y. Hypervalent Iodine Reagents for the Oxidation of Alcohols and Their Application to Complex Molecule Synthesis. *Adv. Synth. Catal.* **2004**, *346*, 111–124. [CrossRef]
3. Zhdankin, V.V.; Stang, P.J. Chemistry of Polyvalent Iodine. *Chem. Rev.* **2008**, *108*, 5299–5358. [CrossRef] [PubMed]
4. Küpper, F.C.; Feiters, M.C.; Olofsson, B.; Kaiho, T.; Yanagida, S.; Zimmermann, M.B.; Carpenter, L.J.; Luther, G.W., III; Lu, Z.; Jonsson, M.; et al. Commemorating Two Centuries of Iodine Research: An Interdisciplinary Overview of Current Research. *Angew. Chem. Int. Ed.* **2011**, *50*, 11598–11620. [CrossRef] [PubMed]
5. Zhdankin, V.V. *Hypervalent Iodine Chemistry: Preparation, Structure, and Synthetic Applications of Polyvalent Iodine Compounds*; Wiley: Chichester, UK, 2013.
6. Yusubov, M.S.; Zhdankin, V.V. Iodine Catalysis: A Green Alternative to Transition Metals in Organic Chemistry and Technology. *Resour.-Effic. Technol.* **2015**, *1*, 49–67. [CrossRef]
7. Yoshimura, A.; Zhdankin, V.V. Advances in Synthetic Applications of Hypervalent Iodine Compounds. *Chem. Rev.* **2016**, *116*, 3328–3435. [CrossRef]
8. Singh, F.V.; Wirth, T. *"Stereoselective Reactions" Patai's Chemistry of Functional Groups*, 1st ed.; John Wiley & Sons, Ltd.: Hoboken, NJ, USA, 2018.

9. Singh, F.V.; Shetgaonkar, S.E.; Krishnan, M.; Wirth, T. Progress in Organocatalysis with Hypervalent Iodine Catalysts. *Chem. Soc. Rev.* **2022**, *51*, 8102–8139. [CrossRef] [PubMed]
10. Dohi, T.; Maruyama, A.; Yoshimura, M.; Morimoto, K.; Tohma, H.; Kita, Y. Versatile Hypervalent-Iodine(III)-Catalyzed Oxidations with *m*-Chloroperbenzoic Acid as a Cooxidant. *Angew. Chem. Int. Ed.* **2005**, *44*, 6193–6196. [CrossRef]
11. Ochiai, M.; Takeuchi, Y.; Katayama, T.; Sueda, T.; Miyamoto, K. Iodobenzene-Catalyzed α-Acetoxylation of Ketones. In Situ Generation of Hypervalent (Diacyloxyiodo)benzenes Using *m*-Chloroperbenzoic Acid. *J. Am. Chem. Soc.* **2005**, *127*, 12244–12245. [CrossRef] [PubMed]
12. Richardson, R.D.; Wirth, T. Hypervalent Iodine Goes Catalytic. *Angew. Chem. Int. Ed.* **2006**, *45*, 4402–4404. [CrossRef]
13. Finkbeiner, P.; Nachtsheim, B.J. Iodine in Modern Oxidation Catalysis. *Synthesis* **2013**, *45*, 979–999. [CrossRef]
14. Rimi; Uttam, B.; Zhdankin, V.V.; Kumar, R. New Isoxazole-Substituted Aryl Iodides: Metal-Free Synthesis, Characterization and Catalytic Activity. *Eur. J. Org. Chem.* **2024**, *27*, e202301191. [CrossRef]
15. Rimi; Soni, S.; Uttam, B.; China, H.; Dohi, T.; Zhdankin, V.V.; Kumar, R. Recyclable Hypervalent Iodine Reagents in Modern Organic Synthesis. *Synthesis* **2022**, *54*, 2731–2748. [CrossRef]
16. Okawara, M.; Mizuta, K. Synthesis and Some Reactions of Polystyrene Iodosoacetate. *Kogyo Kagaku Zasshi* **1961**, *64*, 232–235. [CrossRef]
17. Togo, H.; Sakuratani, K. Polymer-Supported Hypervalent Iodine Reagents. *Synlett* **2002**, *2002*, 1966–1975. [CrossRef]
18. Wang, G.P.; Chen, Z. Hypervalent Iodine in Synthesis XXVIII: The Preparation and Utility of Polymer-Supported Phenyliodine(III) Diacetate. *Synth. Commun.* **1999**, *29*, 2859–2866. [CrossRef]
19. Ley, S.V.; Thomas, A.W.; Finch, H. Polymer-Supported Hypervalent Iodine Reagents in 'Clean' Organic Synthesis with Potential Application in Combinatorial Chemistry. *J. Chem. Soc. Perkin Trans.* **1999**, *1*, 669–671. [CrossRef]
20. Abe, S.; Sakuratani, K.; Togo, H. Synthetic Use of Poly[4-hydroxy(tosyloxy)iodo]styrenes. *J. Org. Chem.* **2001**, *66*, 6174–6177. [CrossRef] [PubMed]
21. Ficht, S.; Mülbaier, M.; Giannis, A. Development of New and Efficient Polymer-Supported Hypervalent Iodine Reagents. *Tetrahedron* **2001**, *57*, 4863–4866. [CrossRef]
22. Tohma, H.; Maegawa, T.; Kita, Y. Facile and Efficient Oxidative Transformation of Primary Alcohols to Methyl Esters in Water Using Hypervalent Iodine(III) Reagents. *Synlett* **2003**, *2003*, 723–725. [CrossRef]
23. Wan, D.-B.; Chen, J.-M. Poly{[4-(Hydroxy)(Tosyloxy)Iodo]Styrene}-Promoted Direct α-Hydroxylation of Ketones to α-Hydroxyketones. *J. Chem. Res.* **2006**, *2006*, 32–33. [CrossRef]
24. Kalberer, E.W.; Whitfield, S.R.; Sanford, M.S. Application of Recyclable Polymer-Immobilized Iodine(III) Oxidants in Catalytic C-H Bond Functionalization. *J. Mol. Catal. A.* **2006**, *251*, 108–113. [CrossRef]
25. Shang, Y.; But, T.Y.S.; Togo, H.; Toy, P.H. Macroporous Polystyrene-Supported (Diacetoxyiodo)benzene: An Efficient Heterogeneous Oxidizing Reagent. *Synlett* **2007**, *2007*, 67–70. [CrossRef]
26. Kumar, A.; Maurya, R.; Ahmad, P.J. Diversity Oriented Synthesis of Benzimidazole and Benzoxa/(thia)zole Libraries through Polymer-Supported Hypervalent Iodine Reagent. *Comb. Chem.* **2009**, *11*, 198–201. [CrossRef] [PubMed]
27. Zhang, J.; Phillips, J.A. The Synthesis and Application of Polymer-Supported Hypervalent Iodine Reagent in the Organic Chemistry Laboratory. *J. Chem. Educ.* **2010**, *87*, 981–984. [CrossRef]
28. Chen, J.-M.; Zeng, X.-M.; Zhdankin, V.V. Preparation and Reactivity of Polystyrene-Supported Iodosylbenzene Sulfate: An Efficient Recyclable Oxidizing System. *Synlett* **2010**, *2010*, 2771–2774. [CrossRef]
29. Qian, W.; Jin, E.; Bao, W.; Zhang, Y. Clean and Highly Selective Oxidation of Alcohols in an Ionic Liquid by Using an Ion-Supported Hypervalent Iodine(III) Reagent. *Angew. Chem. Int. Ed.* **2005**, *44*, 952–955. [CrossRef] [PubMed]
30. Handy, S.T.; Okello, M.J. Homogeneous Supported Synthesis Using Ionic Liquid Supports: Tunable Separation Properties. *Org. Chem.* **2005**, *70*, 2874–2877. [CrossRef]
31. Roy, M.N.; Poupon, J.C.; Charette, A.B. Tetraarylphosphonium Salts as Soluble Supports for Oxidative Catalysts and Reagents. *J. Org. Chem.* **2009**, *74*, 8510–8515. [CrossRef] [PubMed]
32. Zhang, J.; Zhao, D.; Wang, Y.; Kuang, H.; Jia, H. A Facile Synthesis of Ionic Liquid-Supported Iodosylbenzenes. *J. Chem. Res.* **2011**, *35*, 333–335. [CrossRef]
33. Zhu, C.; Yoshimura, A.; Wei, Y.; Nemykin, N.V.; Zhdankin, V.V. Facile Preparation and Reactivity of Bifunctional Ionic Liquid-Supported Hypervalent Iodine Reagent: A Convenient Recyclable Reagent for Catalytic Oxidation. *Tetrahedron Lett.* **2012**, *53*, 1438–1444. [CrossRef]
34. Iinuma, M.; Moriyama, K.; Togo, H. Various Oxidative Reactions with Novel Ion-Supported (Diacetoxyiodo)benzenes. *Tetrahedron* **2013**, *69*, 2961–2970. [CrossRef]
35. Xie, Y.; Pan, H. Regioselective Acetylate of 1,3-Disubstituted Selenoureas Promoted by Recyclable Ion-Supported Hypervalent Iodine(III) Reagent. *Phosphorus Sulfur Silicon Relat. Elem.* **2014**, *189*, 98–105. [CrossRef]
36. Li, X.; Huang, Y.; Gan, B.; Mi, Z.; Xie, Y. Synthesis of Cyanamides from Isoselenocyanates Promoted by Recyclable Ionic Liquid-Supported (Diacetoxyiodo)benzene. *J. Chem. Res.* **2015**, *39*, 631–634. [CrossRef]
37. Rocaboy, C.; Gladysz, J.A. Convenient Syntheses of Fluorous Aryl Iodides and Hypervalent Iodine Compounds: $ArI(L)_n$ Reagents that are Recoverable by Simple Liquid/Liquid Biphase Workups, and Applications in Oxidations of Hydroquinones. *Chem. Eur. J.* **2003**, *9*, 88–95. [CrossRef] [PubMed]

38. Tesevic, V.; Gladysz, J.A. An Easily Accessed Class of Recyclable Hypervalent Iodide Reagents for Functional Group Oxidations: Bis(trifluoroacetate) Adducts of Fluorous Alkyl Iodides, $CF_3(CF_2)_{n-1}I(OCOCF_3)_2$. *Green Chem.* **2005**, *7*, 833–836. [CrossRef]
39. Tesevic, V.; Gladysz, J.A. Oxidations of Secondary Alcohols to Ketones Using Easily Recyclable Bis(trifluoroacetate) Adducts of Fluorous Alkyl Iodides, $CF_3(CF_2)_{n-1}I(OCOCF_3)_2$. *J. Org. Chem.* **2006**, *71*, 7433–7440. [CrossRef] [PubMed]
40. Podgorsek, A.; Jurisch, M.; Stavber, S.; Zupan, M.; Iskra, J.; Gladysz, J.A. Synthesis and Reactivity of Fluorous and Nonfluorous Aryl and Alkyl Iodine(III) Dichlorides: New Chlorinating Reagents that are Easily Recycled using Biphasic Protocols. *J. Org. Chem.* **2009**, *74*, 3133–3140. [CrossRef] [PubMed]
41. Tohma, H.; Maruyama, A.; Maeda, A.; Maegawa, T.; Dohi, T.; Shiro, M.; Morita, T.; Kita, Y. Preparation and Reactivity of 1,3,5,7-Tetrakis[4-diacetoxyiodo)phenyl]adamantane, a Recyclable Hypervalent Iodine(III) Reagent. *Angew. Chem. Int. Ed.* **2004**, *43*, 3595–3598. [CrossRef]
42. Dohi, T.; Maruyama, A.; Yoshimura, M.; Morimoto, K.; Tohma, H.; Shiro, M.; Kita, Y. A Unique Site-Selective Reaction of Ketones with New Recyclable Hypervalent Iodine(III) Reagents Based on a Tetraphenylmethane Structure. *Chem. Commun.* **2005**, *17*, 2205–2207. [CrossRef] [PubMed]
43. Moroda, A.; Togo, H. Biphenyl- and Terphenyl-Based Recyclable Organic Trivalent Iodine Reagents. *Tetrahedron* **2006**, *62*, 12408–12414. [CrossRef]
44. Dohi, T.; Fukushima, K.I.; Kamitanaka, T.; Morimoto, K.; Takanaga, K.; Kita, Y. An Excellent Dual Recycling Strategy for the Hypervalent Iodine/Nitroxyl Radical Mediated Selective Oxidation of Alcohols to Aldehydes and Ketones. *Green Chem.* **2012**, *14*, 1493–1501. [CrossRef]
45. Thorat, P.B.; Bhong, B.Y.; Shelke, A.V.; Karade, N.N. 2,4,6-Tris(4-iodophenoxy)-1,3,5-triazine as a New Recyclable "Iodoarene" for In Situ Generation of Hypervalent Iodine(III) Reagent for α-Tosyloxylation of Enolizable Ketones. *Tetrahedron Lett.* **2014**, *55*, 3332–3335. [CrossRef]
46. Zhu, C.; Wei, Y. Facile Preparation of Magnetic Nanoparticle-Supported Hypervalent Iodine Reagent: A Convenient Recyclable Reagent for Oxidation. *Adv. Synth. Catal.* **2012**, *354*, 313–320. [CrossRef]
47. Shahamat, Z.; Nemati, F.; Elhampour, A. Highly Effective Oxidation of Benzyl Alcohols to Benzaldehydes Over a New Hypervalent Iodine(III) Reagent with the Polymeric Framework and Magnetic Feature as Reusable Heterogeneous Nanocatalyst. *React. Funct. Polym.* **2020**, *146*, 104415. [CrossRef]
48. Nambu, H.; Shimokawa, I.; Fujiwara, T.; Yakura, T. Recyclable Magnetic Nanoparticle-Supported Iodoarene Catalysts for Oxidation of 4-Alkoxyphenols to Quinones. *Asian J. Org. Chem.* **2016**, *5*, 486–489. [CrossRef]
49. Diles, D.C. Recent Advances and Future Directions in Magnetic Materials. *Acta Mater.* **2003**, *51*, 5907–5939. [CrossRef]
50. Polshettiwar, V.; Luque, R.; Fihri, A.; Zhu, H.; Bouhrara, M.; Basset, J.-M. Magnetically Recoverable Nanocatalysts. *Chem. Rev.* **2011**, *111*, 3069–3075. [CrossRef]
51. Gawande, M.J.; Branco, P.S.; Varma, R.S. Nano-Magnetite (Fe_3O_4) as a Support for Recyclable Catalysts in the Development of Sustainable Methodologies. *Chem. Soc. Rev.* **2013**, *42*, 3371–3393. [CrossRef] [PubMed]
52. Baig, R.B.N.; Varma, R.S. Magnetically Retrievable Catalysts for Organic Synthesis. *Chem. Commun.* **2013**, *49*, 752–770. [CrossRef]
53. Mrowczynski, R.; Nan, A.; Liebscher, J. Magnetic Nanoparticle-Supported Organocatalysts—An Efficient Way of Recycling and Reuse. *RSC Adv.* **2014**, *4*, 5927–5952. [CrossRef]
54. Wang, D.; Astruc, D. Fast-Growing Field of Magnetically Recyclable Nanocatalysts. *Chem. Rev.* **2014**, *114*, 6949–6985. [CrossRef] [PubMed]
55. Bushra, R.; Ahmad, M.; Alam, K.; Seidi, F.; Qurtulen; Shakeel, S.; Song, J.; Jin, Y.; Xiao, H. Recent Advances in Magnetic NanoParticles: Key Applications, Environmental Insights, and Future Strategies. *Sustain. Mater. Technol.* **2024**, *40*, e00985. [CrossRef]
56. Gebre, S.H. Recent Developments of Supported and Magnetic Nanocatalysts for Organic Transformations: An Up-To-Date Review. *Appl. Nanosci.* **2023**, *13*, 15–63. [CrossRef]
57. Ovejero, J.G.; Gallo-Cordova, A.; Roca, A.G.; Morales, M.P.; Veintemillas-Verdaguer, S. Reproducibility and Scalability of Magnetic Nanoheater Synthesis. *Nanomaterials* **2021**, *11*, 2059. [CrossRef] [PubMed]
58. Nguyen, M.D.; Deng, L.; Lee, J.M.; Resendez, K.M.; Fuller, M.; Hoijang, S.; Robles-Hernandez, F.; Chu, C.-W.; Litvinov, D.; Hadjiev, V.G.; et al. Magnetic Tunability via Control of Crystallinity and Size in Polycrystalline Iron Oxide Nanoparticles. *Small* **2024**, *20*, 2402940. [CrossRef] [PubMed]
59. Sharma, S.; Sharma, H.; Sharma, R. A Review on Functionalization and Potential Application Spectrum of Magnetic Nanoparticles (MNPs) Based Systems. *Chem. Inorg. Mater.* **2024**, *2*, 100035. [CrossRef]
60. Lu, A.-H.; Salabas, E.L.; Schüth, F. Magnetic Nanoparticles: Synthesis, Protection, Functionalization, and Application. *Angew. Chem. Int. Ed.* **2007**, *46*, 1222–1244. [CrossRef] [PubMed]
61. Feyen, M.; Weidenthaler, C.; Schüth, F.; Lu, A.H. Synthesis of Structurally Stable Collodial Composites as Magnetically Recyclable Acid Catalysts. *Chem. Mater.* **2010**, *22*, 2955–2961. [CrossRef]
62. Mirfakhraei, S.; Hekmati, M.; Eshbala, F.H.; Veisi, H. Fe_3O_4/PEG-SO_3H as a Heterogeneous and Magnetically-Recyclable Nanocatalyst for the Oxidation of Sulfides to Sulfones or Sulfoxides. *New J. Chem.* **2018**, *42*, 1757–1761. [CrossRef]
63. Yang, C.; Wu, J.; Hou, Y. Fe_3O_4 Nanostructures: Synthesis, Growth Mechanism, Properties and Applications. *Chem. Commun.* **2011**, *47*, 5130–5141. [CrossRef]

64. Simeonidis, K.; Liébana-Viñas, S.; Wiedwald, U.; Ma, Z.; Li, Z.-A.; Spasova, M.; Patsia, O.; Myrovali, E.; Makridis, A.; Sakellari, D.; et al. A Versatile Large-Scale and Green Process for Synthesizing Magnetic Nanoparticles with Tunable Magnetic Hyperthermia Features. *RSC. Adv.* **2016**, *6*, 53107–53117. [CrossRef]
65. Maity, D.; Kale, S.N.; Kaul-Ghanekar, R.; Xue, J.-M.; Ding, J. Studies of Magnetite Nanoparticles Synthesized by Thermal Decomposition of Iron(III) Acetylacetonate in Tri(ethylene Glycol). *J. Magn. Magn. Mater.* **2009**, *321*, 3093–3098. [CrossRef]
66. De Palma, R.; Peeters, S.; Van Bael, M.J.; Van den Rul, H.; Bonroy, K.; Laureyn, W.; Mullens, J.; Borghs, G.; Maes, G. Silane Ligand Exchange to Make Hydrophobic Superparamagnetic Nanoparticles Water-Dispersible. *Chem. Mater.* **2007**, *19*, 1821–1831. [CrossRef]
67. Yamamoto, Y.; Togo, H. PhI-Catalyzed α-Tosyloxylation of Ketones with *m*-Chloroperbenzoic Acid and *p*-Toluenesulfonic Acid. *Synlett* **2006**, *2006*, 798–800. [CrossRef]
68. Merritt, E.A.; Olofsson, B. α-Functionalization of Carbonyl Compounds Using Hypervalent Iodine Reagents. *Synthesis* **2011**, *2011*, 517–538. [CrossRef]
69. Moriarty, R.M.; Prakash, O. Oxidation of Phenolic Compounds with Organohypervalent Iodine Reagents. *Org. Reac.* **2001**, *57*, 327–415. [CrossRef]
70. Armarego, W.L.F.; Chai, C.L.L. *Purification of Laboratory Chemicals*, 5th ed.; Elsevier: Oxford UK, 2003.
71. Lucas, H.J.; Kennedy, E.R.; Forno, M.W. Iodosobenzene. *Org. Synth.* **1942**, *22*, 70–71. [CrossRef]
72. Kobayashi, K.; Kondo, Y. Transition-Metal-Free Carboxylation of Organozinc Reagents Using CO_2 in DMF Solvent. *Org. Lett.* **2009**, *11*, 2035–2037. [CrossRef] [PubMed]
73. Everson, D.A.; Shrestha, R.; Weix, D.J. Nickel-Catalyzed Reductive Cross-Coupling of Aryl Halides with Alkyl Halides. *J. Am. Chem. Soc.* **2010**, *132*, 920–921. [CrossRef] [PubMed]
74. Partridge, B.M.; Hartwig, J.F. Sterically Controlled Iodination of Arenes via Iridium-Catalyzed C–H Borylation. *Org. Lett.* **2013**, *15*, 140–143. [CrossRef] [PubMed]
75. Ueno, M.; Nabana, T.; Togo, H. Novel Oxidative α-Tosyloxylation of Alcohols with Iodosylbenzene and p-Toluenesulfonic Acid and Its Synthetic Use for Direct Preparation of Heteroaromatics. *J. Org. Chem.* **2003**, *68*, 6424–6426. [CrossRef] [PubMed]
76. Casey, L.M.; Paulick, R.C.; Whitlock, H.W. Carbon-13 Nuclear Magnetic Resonance Study of the Biosynthesis of Daunomycin and Islandicin. *J. Org. Chem.* **1978**, *43*, 1627–1634. [CrossRef]